ECOLOGICAL SOCIETY OF AMERICA

Ecology/Ecological Monographs/Ecological Applications

PREPRINT

The doi for this manuscript and the correct format for citing the paper are given at the top of the online (html) abstract.

Once the final published version of this paper is posted online, it will replace the preliminary version at the specified doi.

Article type: Report Running head: Nitrogen fixation and metabolic ecology

Does N_2-fixation amplify the temperature dependence of ecosystem metabolism?

Jill R. Welter[1], Jonathan P. Benstead[2], Wyatt F. Cross[3], James M. Hood[3], Alexander D. Huryn[2], Philip W. Johnson[4], and Tanner J. Williamson[3]

[1]Department of Biology, St. Catherine University, Saint Paul, MN 55105, USA

[2]Department of Biological Sciences, University of Alabama, Tuscaloosa, AL 35487, USA

[3]Department of Ecology, Montana State University, Bozeman, MT 59717, USA

[4]Department of Civil, Construction and Environmental Engineering, University of Alabama, Tuscaloosa, AL 35487, USA

Key words: activation energy; amplification; Arrhenius; biofilm; climate change; metabolic theory; nitrogen fixation; nutrient cycling; resource supply; temperature.

ABSTRACT

Variation in resource supply can cause variation in temperature dependences of metabolic processes (e.g., photosynthesis and respiration). Understanding such divergence is particularly important when using metabolic theory to predict ecosystem responses to climate warming. Few studies, however, have assessed the effect of temperature-resource interactions on metabolic processes, particularly in cases where the supply of limiting resources exhibits temperature dependence. We investigated the responses of biomass accrual, gross primary production (GPP), respiration (CR), and N_2-fixation to warming during biofilm development in a streamside channel experiment. Areal rates of GPP, CR, biomass accrual, and N_2-fixation scaled positively with temperature, showing a 32- to 71-fold range across the temperature gradient (~7-24°C). Areal N_2-fixation rates exhibited apparent activation energies (1.5-2.0 eV) approximating the activation energy of the nitrogenase reaction. In contrast, mean apparent activation energies for areal rates of GPP (2.1-2.2 eV) and CR (1.6-1.9 eV) were 6.5 and 2.7-fold higher than estimates based on metabolic theory predictions (i.e., 0.32 and 0.65 eV, respectively) and did not significantly differ from the apparent activation energy observed for N_2-fixation. Mass-specific activation energies for N_2-fixation (1.4-1.6 eV), GPP (0.3-0.5 eV), and CR (no observed temperature relationship) were near or lower than theoretical predictions. We attribute the divergence of areal activation energies from those predicted by metabolic theory to increases in N_2-fixation with temperature, leading to amplified temperature dependences of biomass accrual and areal rates of GPP and R. Such interactions between temperature dependences must be incorporated into metabolic models to improve predictions of ecosystem responses to climate change.

INTRODUCTION

Since 1880, global mean surface temperatures have risen by 0.85°C, and most models predict an increase of ~4°C by 2100 (IPCC 2013). Elevated temperatures have altered the species composition and biogeochemistry of Earth's ecosystems (Grimm et al. 2013), with largely unknown consequences. One of the greatest challenges for this century is to understand and predict how warming will affect the physical, chemical, and biological processes governing ecosystem fluxes of carbon and essential nutrients.

The metabolic theory of ecology (MTE; Brown et al. 2004, Sibly et al. 2012) offers one approach for developing predictions about how temperature influences ecosystem processes. The MTE argues that the relationship between ecosystem metabolism and temperature can be predicted from the temperature dependences of sub-cellular reactions, such as photosynthesis and cellular respiration. The rate of most sub-cellular reactions increases exponentially with temperature following the Van't Hoff-Arrhenius relationship $e^{-E/(kT)}$, where k is the Boltzmann constant (8.61×10^{-5} eV° K^{-1}), T is temperature (°K), and E is the activation energy (AE; units = eV), which quantifies the change in reaction rate with temperature (Boltzmann 1872, Arrhenius 1889). Over a biologically relevant range of temperatures (e.g., 0–30°C), the AEs for respiration and gross primary production for both cells and ecosystems are predicted to be ~0.65 and ~0.32 eV, respectively (Gillooly et al. 2001, Allen et al. 2005). Research in a variety of ecosystems has generally supported this prediction, suggesting that MTE may help forecast ecosystem responses to warming (Enquist et al. 2003, Demars et al. 2011, Perkins et al. 2012,Yvon-Durocher et al. 2012). However, broad application of MTE is currently hindered by a lack of information about how its predictions are influenced by resource supply (Anderson-Teixeira and Vitousek 2012).

Since its conception, there has been considerable effort to incorporate the effects of resource supply into the MTE (Brown et al. 2004, Sterner 2004, Kaspari 2012). Such efforts have been motivated by a growing literature demonstrating both independent and interacting effects of temperature and resource availability on ecosystem processes (Pomeroy and Wiebe 2001, López-Urrutia and Morán 2007, Davidson et al. 2012). Indeed, recent models that explicitly incorporate these factors have refined predictions about how ecosystems respond to global change (e.g., Davidson et al. 2012). Nevertheless, few models incorporate the dynamics of temperature-resource availability relationships.

Rates of many physiological and geochemical processes that control resource supply (e.g., enzyme activity, weathering) increase with temperature (Rennie and Kemp 1986, Bland and Rolls 1998). Thus, warming can increase resource supply, leading to 'apparent' AEs that diverge from canonical (i.e., intrinsic) predictions (Anderson-Teixeira and Vitousek 2012) that are based on temperature alone. Nitrogen (N_2) fixation is one process of particular interest, as it provides an additional source of N to ecosystems (Howarth 1988, Marcarelli et al. 2008, Scott et al. 2009) and has a strong biphasic temperature dependence at the enzymatic level (AE of nitrogenase = 2.18 eV below 22°C, 0.65 eV above 22°C; Ceuterick et al. 1978). As such, increases in N_2-fixation rates with temperature can increase the availability of a limiting resource (i.e., N), potentially leading to temperature dependences of whole-community primary production and respiration that are higher than those predicted by MTE (Anderson-Teixeira et al. 2008). To test this prediction, we experimentally manipulated temperature under strongly N-limited conditions and quantified responses of N_2-fixation, primary production, and community respiration during stream biofilm development.

METHODS

Temperature manipulation and experimental channels

We used experimental stream channels to examine the effect of temperature on biofilms. Our infrastructure was installed in a grassland watershed draining the Hengill volcanic area, 30 km east of Reykjavík, Iceland (064°03′23″N, 021°17′01″W). Hengill is an active geothermal landscape with streams and hot springs that vary in temperature (annual mean temperature range ~6–100°C) due to localized warming (Árnason et al. 1969). Our experimental temperature gradient was achieved using three gravity-fed heat exchangers that were deployed in geothermal pools. These devices heated stream water from an unnamed tributary of Hengladalsá River (mean temperature 7.5°C) to ~10°C and ~20°C above ambient (see Figs. A1 and A2 in Appendix; O'Gorman et al. 2014). Water from the two heat exchangers was then mixed with unheated stream water to produce five water-temperature treatments that were supplied to 15 experimental stream channels (mean °C ± 1 S.D.: 7.5 ± 1.8, 11.2 ± 1.8, 15.5 ± 1.9, 19.0 ± 1.8, 23.6 ± 2.0; $n = 3$ channels per temperature and divided into three blocks with the five temperatures randomized within each block; Table A1 and Fig. A3 in Appendix). The bed of each channel was lined with ~110 25 × 25 mm basalt tiles (Deko Tile, Carson, CA, USA) that were leached in tap water for 18 days and boiled for 5 mins prior to deployment on 20 May 2013. Channels were colonized for 42 days before our first measurement period. We did not prevent macroinvertebrates from colonizing the channels, but very few invertebrates were observed on tiles during the study.

Metabolism and biofilm mass accrual

We measured biofilm metabolism in 0.3 L recirculating chambers constructed from clear Plexiglas® (Fig. A4 in Appendix). Biofilm metabolism, as change in dissolved oxygen (DO) concentration, was measured simultaneously for all treatments within a randomly chosen block

at days 42 and 58. Incubations were typically conducted between 10:00 and 16:00 during sunny conditions.

Each chamber measurement was based on four tiles randomly selected from a single channel. Tiles were sampled without replacement, placed in chambers filled with sieved (250-μm) water from the respective treatment, and incubated in a water bath at the appropriate temperature. We measured net ecosystem production (NEP) under ambient light conditions and community respiration (CR) in the dark. The same tiles were used for both measurements but chamber water was exchanged between measurements. DO and chamber temperatures were recorded at 1-min intervals (YSI Pro-ODO, Yellow Springs, OH, USA). Incubations were terminated after DO changed by >1 mg L^{-1} or at 1.5 hours (average = 1.1 h, range = 0.3-1.7 h). Net ecosystem production and community respiration (mg $DO \cdot m^{-2} \cdot h^{-1}$) were calculated as

$$(NEP) \text{ or } (CR) = \Delta O_2 \cdot V \cdot S^{-1},$$

where ΔO_2 is the slope of the relationship between DO concentration and time (mg $DO \cdot L^{-1} \cdot h^{-1}$), V is chamber volume (L) and S is the active surface area of the tiles (m^2). Gross primary production (GPP) was calculated as: GPP = NEP + CR (Bott 2006). We corrected for water column metabolism by subtracting rates measured in blank chambers without tiles.

Tiles were scrubbed with a toothbrush following incubations and the resulting slurry was aggregated in 125 ml of water in amber bottles. A subsample was then filtered onto a pre-ashed, Whatman GF/F filter, dried (55°C, ≥72 hrs), weighed and ashed at 500°C for two hours and reweighed to determine biomass as ash-free dry mass (AFDM). Biomass accrual (mg $AFDM \cdot m^{-2} \cdot day^{-1}$) was calculated as the mean channel AFDM divided by days incubated.

Nitrogen fixation

136 N_2-fixation rates were measured using acetylene reduction assays (Flett et al. 1976, Capone
137 1993) during 2-h mid-day incubations at 41 and 53 days post-deployment, using the sampling
138 design and chambers described above. Twenty ml of acetylene gas was injected directly into
139 each chamber and mixed vigorously for 5-min prior to incubation. Gas samples were collected
140 from each chamber at the beginning and end of the incubation. All gas samples, including field
141 standards, were analyzed for ethylene concentration on an SRI 8610 gas chromatograph with a
142 flame ionization detector (Hayesep T column, 80/100 mesh) within 48 hours of collection. The
143 rate of ethylene production in each chamber was calculated and a 3:1 N_2:ethylene conversion
144 ratio (Capone 1993) was used to estimate N_2-fixation rates.

145 *Activation energies and statistical analysis*

146 AEs were estimated for areal and mass-specific rates of GPP, CR, N_2-fixation, and
147 biomass accrual using the Van't Hoff-Arrhenius relationship. We used linear least-squares
148 regression to fit a relationship between $\log_e$-transformed process rates and $1/kT$ (R Core Team
149 2013). The AE is the absolute value of the slope; 95% confidence intervals were calculated with
150 the 'confint' function in the R package 'stats' (R Core Team 2013). We tested for differences in
151 AE among GPP, N_2-fixation, and CR, as well as between areal and mass-specific rates, using a
152 linear model that predicted flux rate using $1/kT$ and the flux identity. A significant ($\alpha = 0.05$)
153 interaction between $1/kT$ and the flux type indicated a significant difference among slopes. The
154 mean channel temperature prior to the sampling day was used to calculate the AE of biomass
155 accrual, while mean chamber incubation temperatures were used for the other flux measurements.
156 Incubation temperatures during GPP, CR, and N_2-fixation measurements were strongly related to
157 mean channel temperature prior to the sampling date ($°C_{incubation} = 4.04 + 0.81°C_{channel}$; $R^2 = 0.92$,

158 $P < 0.001$); however, incubation temperatures were slightly warmer because incubations
159 generally occurred near maximum daily temperature (Fig. A5 in Appendix).

160 To assess whether temperature or biomass best predicted ecosystem flux rates, we first
161 compared the AEs of mass-specific and areal GPP and CR to canonical expectations. Second, we
162 used repeated measures mixed-effects models ('lme' function in the R package 'nlme'; fixed
163 effects = sampling day and either $1/kT$ or $\log_e$ biomass, random intercept = channel ID, random
164 slope = sampling day) and compared resulting AICc scores (Burnham & Anderson 2002) to
165 identify whether temperature ($1/kT$) or biomass ($\log_e$-transformed AFDM) best predicted $\log_e$
166 areal GPP and CR. Tests for multicollinearity indicated a strong correlation between temperature
167 and biomass (e.g., for areal GPP: $R^2 = 0.79$, $P < 0.001$); thus, we used a model selection
168 approach to examine models containing only one of these terms.

169 RESULTS

170 Our temperature manipulations were effective and relatively consistent throughout the
171 experiment (Table A1 and Fig. A5 in Appendix). The daily ranges of temperature were similar
172 both among treatments (Table A1) and to those observed in nearby streams (W. F. Cross and J. P.
173 Benstead, *unpublished data*). Biofilm mass accrual was strongly and positively related to
174 temperature, varying on average ~18-fold over the 17°C range in mean temperature (Fig. 1a and
175 Table 1). Areal rates of GPP, CR, and N_2-fixation were also strongly and positively related to
176 temperature. Areal rates of GPP varied on average 53-fold across the treatments on both
177 measurement dates, while areal rates of CR and N_2-fixation varied on average 32- and 71-fold,
178 respectively. On both measurement dates, apparent AEs for the different flux rates (i.e., areal
179 GPP, CR, and N_2-fixation) were statistically indistinguishable (P values > 0.2). Mean apparent
180 AEs for areal GPP and CR were 6.5 and 2.7-fold higher than values predicted by MTE on both

measurement days (Fig. 1 and Table 1). In contrast, the AE of areal N_2-fixation rates, although more variable across measurements, was similar to expectations (Fig. 1d and Table 1) based on the AE of nitrogenase when isolated in the laboratory (2.18 eV below 22°C; Ceuterick et al. 1978).

In contrast to areal rates, the AEs of mass-specific rates differed among flux types ($P < 0.05$). Mass-specific GPP varied 3.8-fold across the thermal gradient and showed a relatively weak positive relationship ($P = 0.065$) with temperature (Fig. 2a and Table 1). The apparent AE of mass-specific GPP approached canonical expectations (i.e., 0.32 eV; Fig. 1a and Table 1) and was much lower than that of areal GPP (both dates: $P < 0.001$). Mass-specific CR rates were not related to temperature (Fig. 2b) and strongly differed from that of areal CR (both dates: $P < 0.001$). Mass-specific N_2-fixation rates increased ~36-fold over the 17°C range and showed mean apparent AEs (i.e., 1.39 eV at day 41 and 1.64 eV at day 53) that were similar to AEs for areal N_2-fixation rates (both dates: $P > 0.05$). Models that contained temperature, rather than biomass, best predicted both areal GPP (temperature model AICc = 38.9, biomass model AICc = 41.8) and areal CR (temperature model AICc = 38.7, biomass model AICc = 47.1); however, models predicting ecosystem flux rates using only biomass still performed exceptionally well (Table A2 in Appendix).

DISCUSSION

Our experiment revealed several patterns in the relationships between temperature and the development and metabolic activity of stream biofilms. Chief among these was the frequent divergence of apparent areal AEs from their expected canonical values. In our study, amplification of the apparent AEs for biomass accrual, and areal GPP and CR, was associated with the dominance of N_2-fixers, a key functional group, which developed across the temperature

gradient (>90% of total biomass in all treatments was comprised of N_2-fixers; Williamson 2014). This can be explained by the high canonical AE of N_2-fixation compared with GPP and CR, which results in substantive increases in N supply and, therefore, metabolic activity associated with reduced N limitation of GPP and biomass accrual along the temperature gradient. Although such amplification has been described in terrestrial systems, typically in the context of soil carbon decomposition (Davidson and Janssens 2006, Yvon-Durocher et al. 2012) or forest primary succession (Anderson-Teixeira et al. 2008), our study highlights the potential for N_2-fixation to also amplify the temperature dependence of ecosystem processes.

Our hypothesis that amplified AEs of areal GPP and CR are driven by increased N supply is supported by the patterns in N_2-fixation measured in our experiment. Areal N_2-fixation rates exhibited an AE that was close to expectations for the nitrogenase enzyme (i.e., 2.18 eV below 22°C, 0.65 eV above 22°C; Ceuterick et al. 1978), while the temperature dependences of GPP and CR were much higher than canonical values (i.e, AE for areal GPP: 2.11-2.15 eV vs. canonical value of 0.33 eV; AE for CR: 1.60-1.86 eV vs. canonical value of 0.60-0.70; Allen et al. 2005). Importantly, the apparent AEs of areal GPP and CR paralleled that of N_2-fixation, suggesting the observed amplification of GPP and CR was driven by a new source of N supplied by elevated rates of N_2-fixation at warm temperatures. This interpretation is consistent with a growing body of literature demonstrating that temperature dependences of resource supply rates can influence the response of ecosystem processes to warming (Anderson-Teixeira et al. 2008, Yvon-Durocher et al. 2012). In essence, the AE of the supply rate of the limiting resource should dictate the apparent AEs of GPP and CR. Thus, in N-poor environments, we might expect significant amplification of ecosystem metabolism in response to warming when N_2-fixers dominate.

Amplified temperature dependences observed in our study could result from two different, non-mutually exclusive, mechanisms. First, temperature could directly influence sub-cellular rates of N_2-fixation, resulting in higher N supply and subsequent increases in rates of photosynthesis and cellular respiration on a per-cell basis (e.g., Rhee and Gotham 1981, Robarts and Zohary 1987). Such a response should be reflected in amplified AEs of mass-specific rates of GPP and CR. Second, increased temperature and N supply (via N_2-fixation) could amplify rates of biomass accrual, based simply on the addition of more metabolically-active cells per area. While the strong correlation between temperature and biomass observed in our study ($R^2 = 0.79$, $P < 0.001$) precludes us from clearly distinguishing these direct (sub-cellular reactions) and indirect (biomass accrual) effects, the strongly amplified AEs of areal GPP and CR versus the AEs of mass-specific rates, which encompassed canonical expectations (e.g., AE for mass-specific GPP: 0.27-0.47 eV), suggests that biomass accrual was a key driver of the amplified response. Such indirect effects of temperature have been largely underappreciated but may help explain why temperature *per se* may not directly predict large-scale patterns of primary production (e.g., Michaletz et al. 2014).

It is possible that amplified temperature dependence of biomass accrual alone can lead to higher ecosystem-level AEs for metabolism, but results from previous studies are mixed. For instance, Anderson-Teixeira et al. (2008) showed that amplified temperature dependence of forest primary succession resulted, in part, from positive effects of warming on accrual and storage of soil and leaf biomass. In contrast, Yvon-Durocher et al. (2010, 2011) demonstrated that warming actually reduced storage of photosynthetic biomass in experimental ponds, while biomass accrual (as net primary production) roughly followed MTE predictions (AE = 0.41 eV). Such discrepancies may be explained by how temperature influences the supply rate of limiting

nutrients or 'reactants', as well as how nutrients are utilized and stored (e.g., assimilation and cell stoichiometry), or transformed (e.g., dissimilatory processes) as they become available. Our study indicates that warming may elevate N_2-fixation in aquatic systems and alleviate N-limitation of biomass accrual, leading to amplified temperature dependence of metabolism in stream biofilms. However, whether or not this amplification also occurs at the whole stream scale depends on the total flux and fate of N introduced to the ecosystem from N_2-fixation. Interestingly, previous measurements of whole-stream metabolism across a natural thermal gradient in the Hengill area (Demars et al. 2011) showed that AEs of GPP and ER were not amplified, but relatively close to MTE predictions, suggesting that the temperature-dependent N supplement to the biofilm is either not sufficient to amplify metabolism at the ecosystem scale or it is unaccounted for in whole-stream metabolism as a result of increases in N loss via denitrification, downstream export, or transfer to the terrestrial environment.

In contrast to patterns in areal fluxes, the AEs of mass-specific flux rates were often near or lower than predictions based on MTE. We attribute these results to the differential rate of biofilm accrual across the experimental temperature gradient and its effect on biofilm thickness and associated shifts in cell physiology. The negative effect of biofilm thickness on mass-specific process rates is well documented, with potential mechanisms including self-shading and limitation by nutrients or inorganic carbon supply (Lamberti and Resh 1983). Such limitation would have become progressively more severe with warming in our experiment, as cells deep in the biofilm experienced reduced access to resources, including light. The suppression of temperature dependence due to resource limitation of cell activity in the higher temperature treatments, where biofilm biomass was high, is consistent with our hypothesis of amplified temperature dependences of areal rates being driven by increased N supply.

Although anthropogenic N inputs have significantly altered N cycling on a global scale (Galloway et al. 2008), the supply of N – in addition to phosphorus – can still limit productivity in terrestrial, marine and freshwater ecosystems worldwide (Smith et al. 1999, Elser et al. 2007, LeBauer and Treseder 2008). Thus, amplified responses of ecosystem metabolism to warming, in response to increased N_2-fixation, could conceivably be widespread. The ability to scale-up or otherwise extrapolate the results of our experiment to different systems is difficult, however, because despite the high AE of nitrogenase activity (Ceuterick et al. 1978), empirical estimates of the AE of N_2-fixation are quite variable (e.g., Brouzes and Knowles 1973, Kashyap et al. 1991), potentially due to intrinsic factors such as temperature-dependent resource limitation of N_2-fixation itself (e.g., by phosphorus, iron, or molybdenum). Nevertheless, amplified responses of ecosystem metabolism to warming may be significant worldwide, but particularly within the acutely nutrient-limited ecosystems of the Arctic and sub-Arctic, where warming is expected to be most severe (e.g., Slavik et al. 2004, Weintraub and Schimel 2005).

ACKNOWLEDGMENTS

This study was funded by the National Science Foundation (DEB-0949774 and DEB-0949726) and additional support from St. Catherine University to J. R. Welter. We thank Chau Tran for assisting in the construction of the heat exchangers, and undergraduate students Aimee Ahles, Jackie Goldschmidt, and Ellie Zignego for their collaboration in the development of methods and assistance with all field and laboratory work associated with this project. We also thank Jón Ólafsson, Gísli Már Gíslason, and the scientists and staff at the Institute of Freshwater Fisheries in Iceland for their knowledge, support, and laboratory facilities that made this work possible.

LITERATURE CITED

295 Allen, A. P., J. F. Gillooly, and J. H. Brown. 2005. Linking the global carbon cycle to individual
296 metabolism. Functional Ecology 19:202-213.
297 Anderson-Teixeira, K. J., P. M. Vitousek, and J. H. Brown. 2008. Amplified temperature
298 dependence in ecosystems developing on the lava flows of Mauna Loa, Hawai'i. Proceedings
299 of the National Academy of Sciences 105:228-223.
300 Anderson-Teixeira, K. J., and P. M. Vitousek. 2012. Ecosystems. Pages 99-111 in R. M. Sibly, J.
301 H. Brown, and A. Kodric-Brown, eds. Metabolic ecology. Wiley-Blackwell, London, U.K.
302 Árnason, B., P. Theodorsson, S. Björnsson, and K. Saemundsson. 1969. Hengill, a high
303 temperature thermal area in Iceland. Bulletin of Volcanology 33:245-259.
304 Arrhenius, S. 1889. Über die Reaktionsgeschwindigkeit bei der Inversion von Rohrzucker durch
305 Säuren. Zeitschrift für Physikalische Chemie 4:266-248.
306 Bland, W., and D. Rolls. 1998. Weathering. Arnold, London, U.K.
307 Boltzmann, L. 1872. Weitere Studien über das Wärmegleichgewicht unter Gasmolekülen.
308 Sitzungsberichte der kaiserlichen Akademie der Wissenschaften 66:275-370.
309 Bott, T. 2006. Primary production and community respiration *in* F. Hauer and G. Lamberti,
310 editors. Methods in stream ecology. Elsevier, New York.
311 Brouzes, R. and R. Knowles. 1973. Kinetics of nitrogen fixation in a glucose-amended,
312 anaerobically incubated soil. Soil Biology and Biochemistry 5:223-229.
313 Brown, J. H., J. F. Gillooly, A. P. Allen, V. M. Savage, and G. B. West. 2004. Toward a
314 metabolic theory of ecology. Ecology 85:1771-1789.
315 Capone, D. G. 1993. Determination of nitrogenase activity in aquatic samples using the
316 acetylene reduction procedure. Pages 621-623 *in* P. F. Kemp, B. F. Sherr, E. B. Sherr, and J.
317 J. Cole, editors. Handbook of methods in microbial ecology. Lews Publishers, Chelsea, MI.

Ceuterick, F., J. Peeters, K. Heremans, H. De Smedt, and H. Olbrechts. 1978. Effect of high pressure, detergents and phospholipase on the break in the Arrhenius plot of *Azotobacter* nitrogenase. European Journal of Biochemistry 87:401-407.

Davidson, E. A., and I. A. Janssens. 2006. Temperature sensitivity of soil carbon decomposition and feedbacks to climate change. Nature 440:165-173.

Davidson, E. A., S. Samanta, S. S. Caramori, and K. Savage. 2012. The Dual Arrhenius and Michaelis-Menten kinetics model for decomposition of soil organic matter at hourly to seasonal time scales. Global Change Biology 18:371-384.

Demars, B. O. L., J. R. Manson, J. S. Ólafsson, G. M. Gíslason, R. Gudmundsdóttir, G. Woodward, J. Reiss, D. E. Pichler, J. J. Rasmussen, and N. Friberg. 2011. Temperature and the metabolic balance of streams. Freshwater Biology 56:1106-1121.

Elser, J. J., M. E. S. Bracken, E. E. Cleland, D. S. Gruner, W. S. Harpole, H. Hillebrand, J. T. Ngai, E. W. Seabloom, J. B. Shurin, and J. E. Smith. 2007. Global analysis of nitrogen and phosphorus limitation of primary producers in freshwater, marine and terrestrial ecosystems. Ecology Letters 10:1135-1142.

Enquist, B. J., E. P. Economo, T. E. Huxman, A. P. Allen, D. D. Ignace, and J. F. Gillooly. 2003. Scaling metabolism from organisms to ecosystems. Nature 423:639-642.

Flett, R. J., R. D. Hamilton, and N. E. R. Campbell. 1976. Aquatic acetylene-reduction techniques: solutions to several problems. Canadian Journal of Microbiology 22:43-51.

Galloway, J. N., A. R. Townsend, J. W. Erisman, M. Bekunda, Z. Cai, J. R. Freney, L. A. Martinelli, S. P. Seitzinger, and M. A. Sutton. 2008. Transformation of the nitrogen cycle: recent trends, questions, and potential solutions. Science 320:889-892.

340 Gillooly, J. F., J. H. Brown, G. B. West, V. M. Savage, and E. L. Charnov. 2001. Effects of size
341 and temperature on metabolic rate. Science 293:2248-2251.
342 Grimm, N. B., and 11 co-authors. 2013. The impacts of climate change on ecosystem structure
343 and function. Frontiers in Ecology and the Environment 11:474-482.
344 Howarth, R. W. 1988. Nutrient limitation of net primary production in marine ecosystems.
345 Annual Review of Ecology and Systematics 19:89-110.
346 IPCC. 2013. Climate change 2013: the physical science basis. Contribution of Working Group I
347 to the Fifth Assessment Report of the Intergovernmental Panel on Climate Change.
348 Cambridge University Press, Cambridge, United Kingdom and New York, NY, USA.
349 Kashyap, A. K., K. D. Pandey, and R. K. Gupta. 1991. Nitrogenase activity of the Antarctic
350 cyanobacterium *Nostoc commune*: influence of temperature. Folia Microbiologica 36:557-
351 560.
352 Kaspari, M. 2012. Stoichiometry *in* R. M. Sibly, J. H. Brown, and A. Kodric-Brown, editors.
353 Metabolic ecology. Wiley-Blackwell, U.K.
354 Lamberti, G. A., and V. H. Resh. 1983. Stream periphyton and insect herbivores: an
355 experimental study of grazing by a caddisfly population. Ecology 64:1124-1135.
356 LeBauer, D.S., and K. K. Treseder. 2008. Nitrogen limitation of net primary productivity in
357 terrestrial ecosystems is globally distributed. Ecology 89:371-379.
358 López-Urrutia, A., and X. A. Morán. 2007. Resource limitation of bacterial production distorts
359 the temperature dependence of oceanic carbon cycling. Ecology 88:817-822.
360 Marcarelli, A. M., M. A. Baker, and W. A. Wurtsbaugh. 2008. Is in-stream N_2 fixation an
361 important N source for benthic communities in stream ecosystems? Journal of the North
362 American Benthological Society 27:186-211.

363 Michaletz, S. T., D. Cheng, A. J. Kerkhoff, and B. J. Enquist. 2014. Convergence of terrestrial
364 plant production across global climate gradients. Nature 512:39-43.
365 O'Gorman, E. J. O, J. P. Benstead, W. F. Cross, N. Friberg, J. M. Hood, P. W. Johnson, B. D.
366 Sigurdsson, and G. Woodward. 2014. Climate change and geothermal ecosystems: natural
367 laboratories, sentinel systems, and future refugia. Global Change Biology
368 doi:10.1111/gcb.12602.
369 Perkins, D. M., G. Yvon-Durocher, B. O. L. Demars, J. Reiss, D. E. Pichler, N. Friberg, M.
370 Trimmer, and G. Woodward. 2012. Consistent temperature dependence of respiration across
371 ecosystems contrasting in thermal history. Global Change Biology 18:1300-1311.
372 Pomeroy, L. R., and W. J. Wiebe. 2001. Temperature and substrates as interactive limiting
373 factors for marine heterotrophic bacteria. Aquatic Microbial Ecology 23:187-204.
374 R Core Team. 2013. R: A language and environment for statistical computing. R Foundation for
375 Statistical Computing, Vienna, Austria.
376 Rennie, R. J., and G. A. Kemp. 1986. Temperature-sensitive nodulation and N_2 fixation of
377 *Rhizobium leguminosarum* biovar *phaseoli* strains. Canadian Journal of Soil Science 66:217-
378 224.
379 Rhee G-Y., and I. J. Gotham. 1981. The effect of environmental factors on phytoplankton
380 growth: temperature and the interactions of temperature with nutrient limitation. Limnology
381 and Oceanography 26: 635-648.
382 Robarts, R. D., and T. Zohary. 1987. Temperature effects on photosynthetic capacity, respiration,
383 and growth rates of bloom-forming cyanobacteria. New Zealand Journal of Marine and
384 Freshwater Research 21:391-399.
385 Scott, J. T., D. A. Lang, R. S. King, and R. D. Doyle. 2009. Nitrogen fixation and phosphatase

activity in periphyton growing on nutrient diffusing substrata: evidence for differential nutrient limitation of stream periphyton. Journal of the North American Benthological Society 28:57-68.

Sibly, R. M., J. H. Brown, and A. Kodric-Brown. 2012. Metabolic ecology. Wiley-Blackwell, U.K.

Slavik, K., B. J. Peterson, L. A. Deegan, W. B. Bowden, A. E. Hershey, and J. E. Hobbie. 2004. Long-term responses of the Kuparuk River ecosystem to phosphorus fertilization. Ecology 85:939-954.

Smith, V. H., G. D. Tilman, and J. C. Nekola. 1999. Eutrophication: impacts of excess nutrient inputs on freshwater, marine, and terrestrial ecosystems. Environmental Pollution 100:179-196.

Sterner, R. W. 2004. A one-resource "stoichiometry"? Ecology 85:1813-1816.

Weintraub, M. N., and J. P. Schimel. 2005. Nitrogen cycling and the spread of shrubs control changes in the carbon balance of arctic tundra ecosystems. BioScience 55:408-415.

Williamson, T. J. 2014. Coupling energy and elements in a warming world: how temperature shapes biofilm ecosystem structure and function. M.S. Thesis, Department of Ecology, Montana State University.

Yvon-Durocher, G., and 11 co-authors. 2012. Reconciling the temperature dependence of respiration across timescales and ecosystem types. Nature 487:472-476.

Yvon-Durocher, G., J. I. Jones, M. Trimmer, G. Woodward, and J. M. Montoya. 2010. Warming alters the metabolic balance of ecosystems. Philosophical Transactions of the Royal Society B 365:2117-2126.

410 Appendix A. Detailed temperature manipulation and experimental channel methods description

411 and statistical output from mixed-effects model selection.

412 Table 1. Estimates of the intercept (SE), slope (SE), *P*-value, and R^2 from least-squared regression of the relationship between several $\log_e$-transformed measures and kT^{-1}. The apparent activation energy for each measure is the product of -1 and the slope.

Measure	Units	Day	Intercept	Slope	*P*-value	R^2
Areal rates						
Biofilm mass accrual	mg AFDM m^{-2} day^{-1}	42	59.1 (5.91)	-1.34 (0.15)	< 0.001	0.86
Biofilm mass accrual	mg AFDM m^{-2} day^{-1}	58	58.28 (3.36)	-1.32 (0.08)	< 0.001	0.95
Gross primary production	mg O_2 m^{-2} hr^{-1}	42	88.68 (10.09)	-2.11 (0.25)	< 0.001	0.87
Gross primary production	mg O_2 m^{-2} hr^{-1}	58	91.26 (6.15)	-2.15 (0.15)	< 0.001	0.95
Respiration	mg O_2 m^{-2} hr^{-1}	42	67.24 (6.39)	-1.60 (0.16)	< 0.001	0.90
Respiration	mg O_2 m^{-2} hr^{-1}	58	78.17 (9.44)	-1.86 (0.24)	< 0.001	0.85
N_2-fixation	mg N_2 m^{-2} hr^{-1}	41	62.89 (8.52)	-1.57 (0.21)	< 0.001	0.81
N_2-fixation	mg N_2 m^{-2} hr^{-1}	53	81.57 (13.55)	-2.04 (0.34)	< 0.001	0.74
Mass-specific rates						

Gross primary production	mg O_2 mg AFDM^{-2} hr^{-1}	42	14.00 (9.05)	-0.47 (0.23)	0.065	0.30
Gross primary production	mg O_2 mg AFDM^{-2} hr^{-1}	58	6.70 (7.12)	-0.27 (0.18)	0.065	0.18
Respiration	mg O_2 mg AFDM^{-2} hr^{-1}	42	-3.3 (7.06)	-0.07 (0.18)	0.712	0.01
Respiration	mg O_2 mg AFDM^{-2} hr^{-1}	58	-0.88 (8.33)	-0.13 (0.21)	0.555	0.03
N_2-fixation	mg N_2 mg AFDM^{-2} hr^{-1}	41	46.81 (16.3)	-1.39 (0.4)	0.004	0.48
N_2-fixation	mg N_2 mg AFDM^{-2} hr^{-1}	53	56.47 (22.04)	-1.64 (0.55)	0.011	0.41

414

FIGURE LEGENDS

Figure 1. Temperature dependence of (a) biomass, (b) gross primary production, (c) community respiration, and (d) N_2-fixation plotted as the relationship between $\log_e$-transformed biomass or areal rates and inverse temperature ($1/kT$). The estimated activation energy (eV) and 95% confidence interval are displayed for each measurement and sampling day when the slope differed significantly from zero ($\alpha = 0.10$). Lines were fit with least-squared regression.

Figure 2. The temperature dependence of mass-specific rates of (a) gross primary production, (b) community respiration, and (c) N_2-fixation plotted as the relationship between $\log_e$-transformed rates and inverse temperature ($1/kT$). The estimated activation energy (eV) and 95% confidence interval are displayed for each measurement and sampling day when the slope differed significantly from zero ($\alpha = 0.10$). Lines were fit with least-squared regression. Mass-specific respiration rates were not related to temperature.

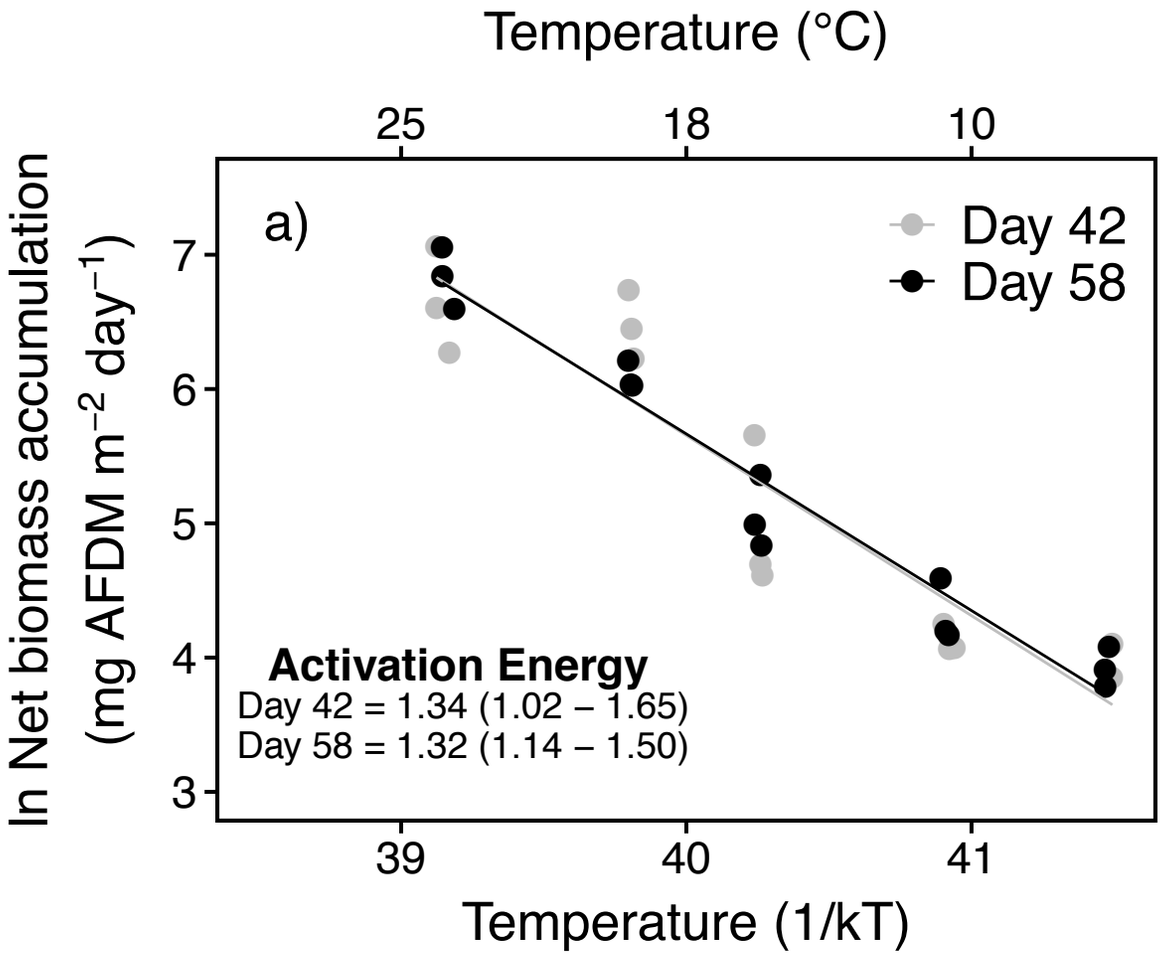
Temperature (°C)
25
18
10
a)
Day 42
Day 58
ln Net biomass accumulation
(mg AFDM m^{-2} day^{-1})
7
6
5
4
3
Activation Energy
Day 42 = 1.34 (1.02 – 1.65)
Day 58 = 1.32 (1.14 – 1.50)
39
40
41
Temperature (1/kT)

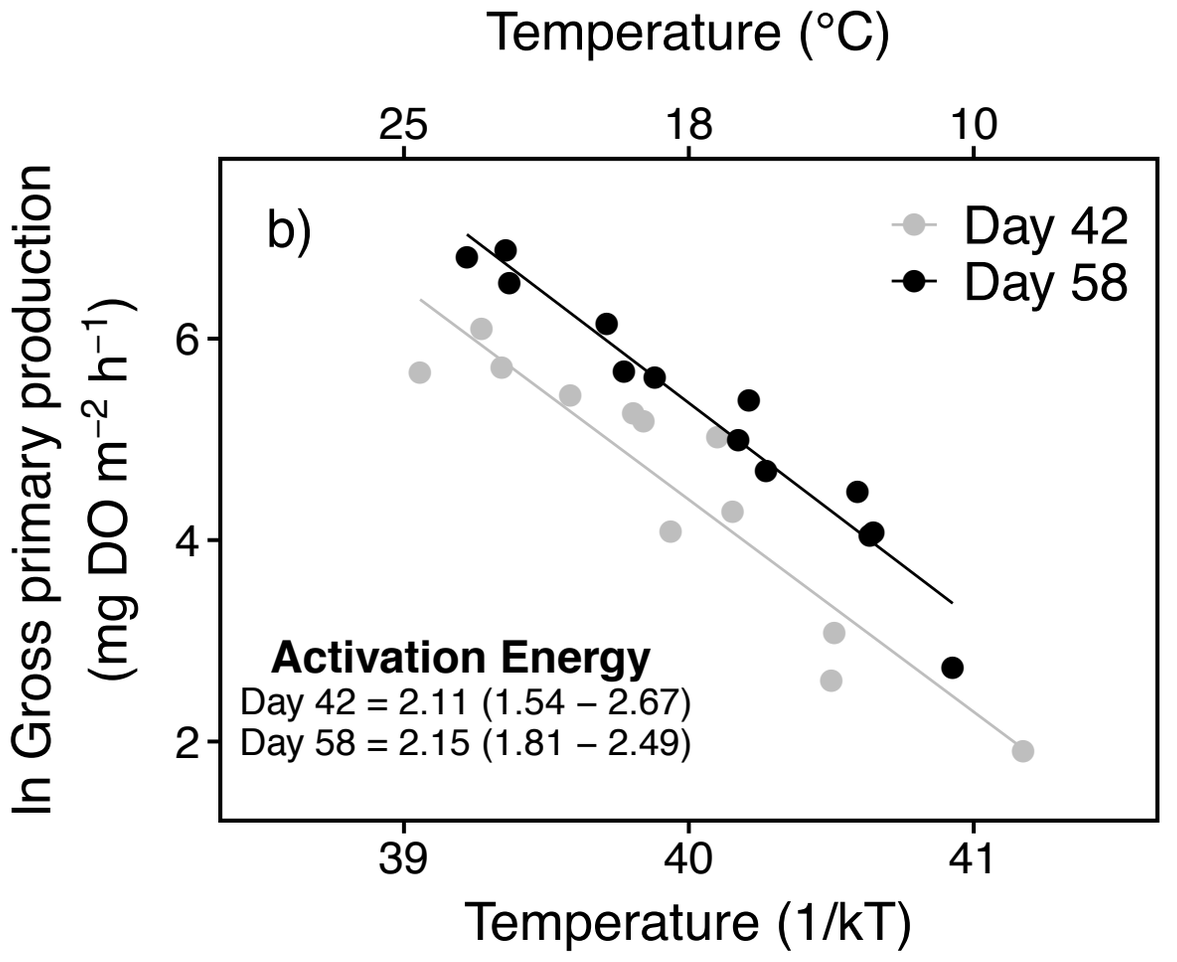
Temperature (°C)
25
18
10
b)
Day 42
Day 58
ln Gross primary production
(mg DO m^{-2} h^{-1})
6
4
2
Activation Energy
Day 42 = 2.11 (1.54 – 2.67)
Day 58 = 2.15 (1.81 – 2.49)
39
40
41
Temperature (1/kT)

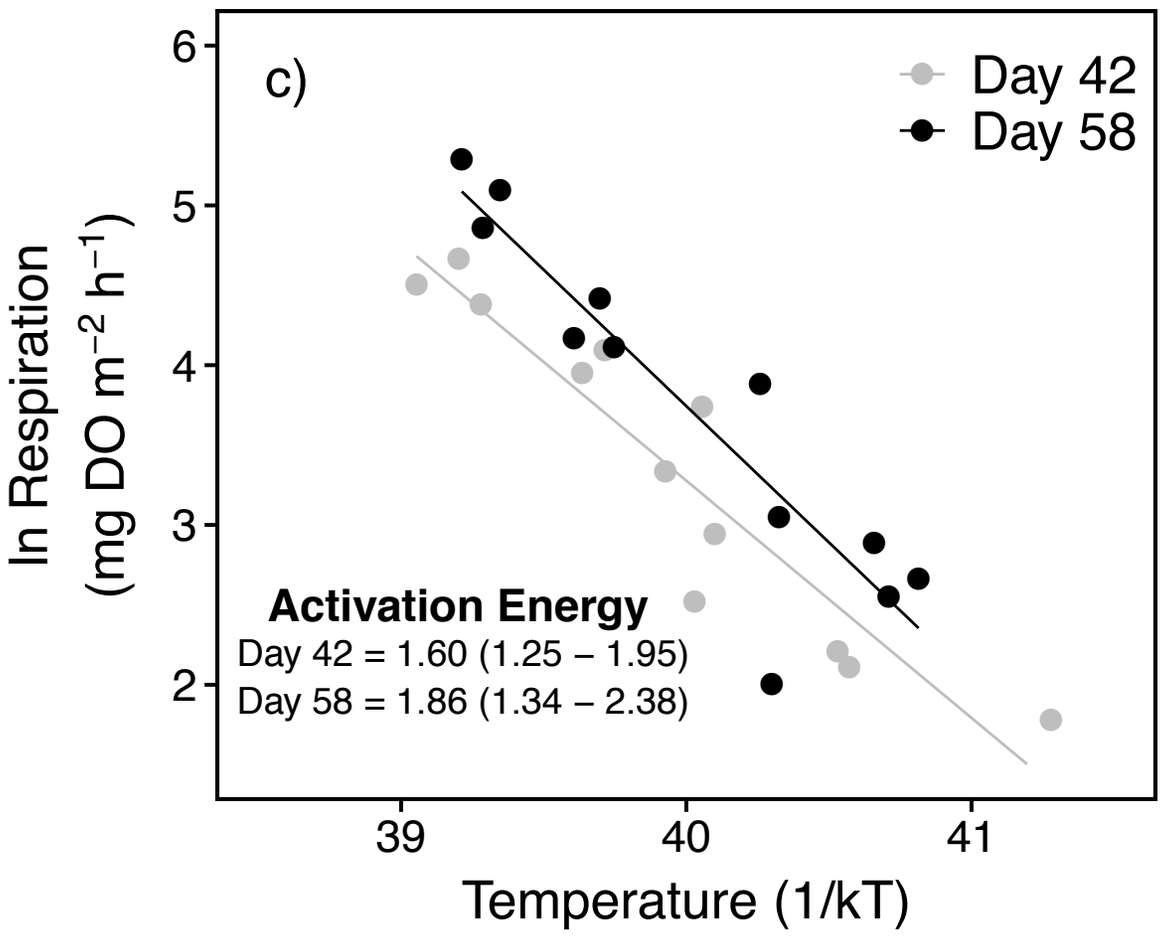
c)
Day 42
Day 58
ln Respiration
(mg DO m^{-2} h^{-1})
6
5
4
3
2
Activation Energy
Day 42 = 1.60 (1.25 – 1.95)
Day 58 = 1.86 (1.34 – 2.38)
39
40
41
Temperature (1/kT)

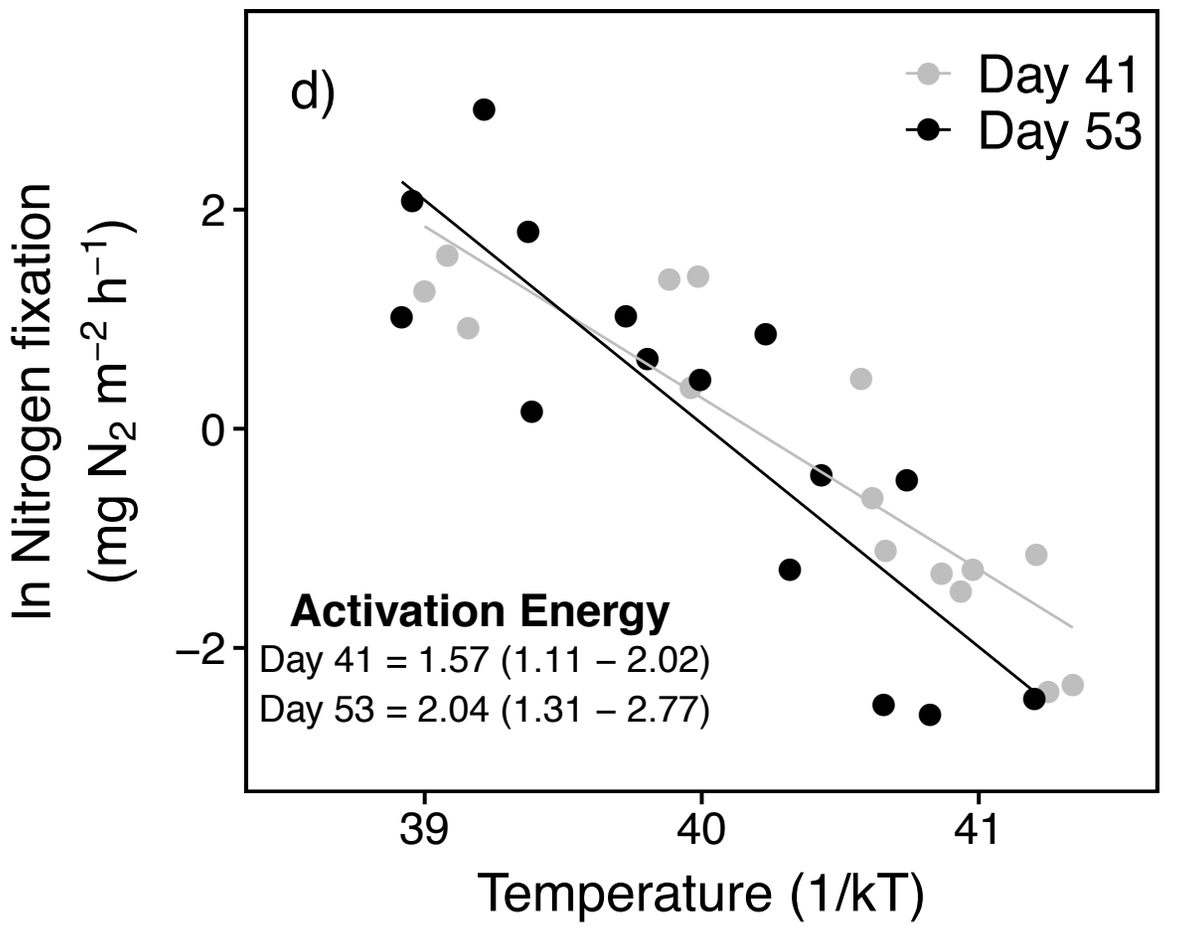
d)
Day 41
Day 53
ln Nitrogen fixation
(mg N_2 m^{-2} h^{-1})
2
0
−2
Activation Energy
Day 41 = 1.57 (1.11 – 2.02)
Day 53 = 2.04 (1.31 – 2.77)
39
40
41
Temperature (1/kT)

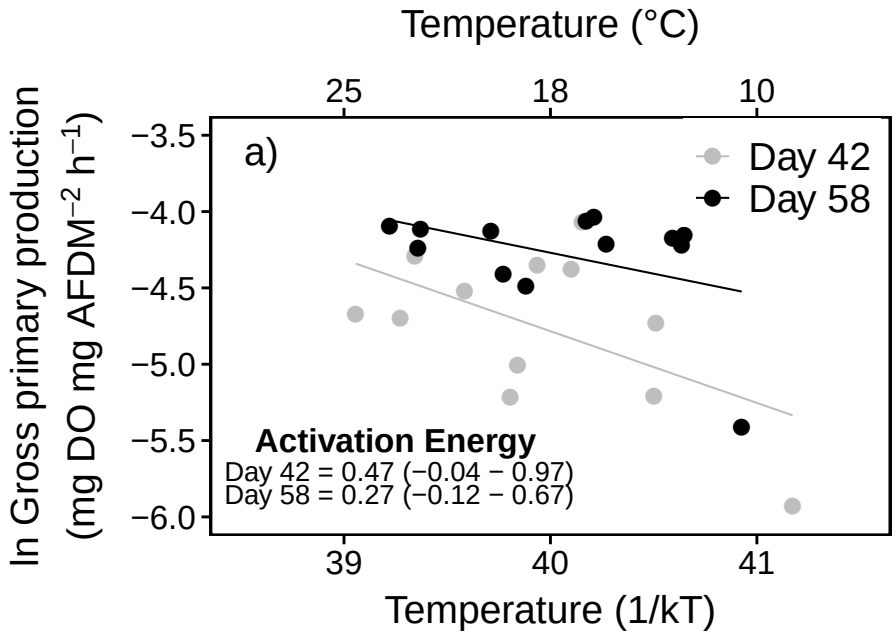
Temperature (°C)
25
18
10
a)
Day 42
Day 58
ln Gross primary production
(mg DO mg AFDM^{-2} h^{-1})
−3.5
−4.0
−4.5
−5.0
−5.5
−6.0
Activation Energy
Day 42 = 0.47 (−0.04 − 0.97)
Day 58 = 0.27 (−0.12 − 0.67)
39
40
41
Temperature (1/kT)

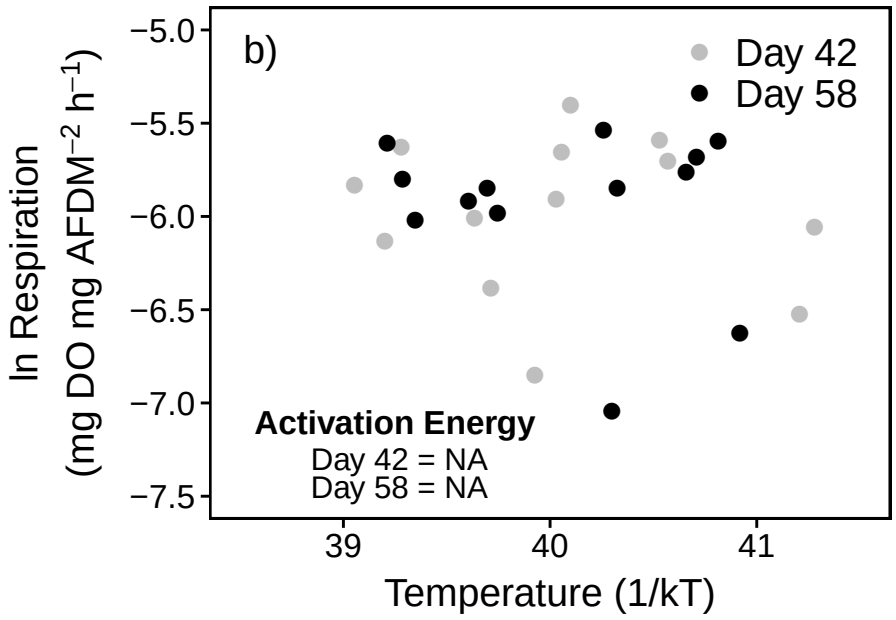
b)
Day 42
Day 58
ln Respiration
(mg DO mg AFDM^{-2} h^{-1})
−5.0
−5.5
−6.0
−6.5
−7.0
−7.5
Activation Energy
Day 42 = NA
Day 58 = NA
39
40
41
Temperature (1/kT)

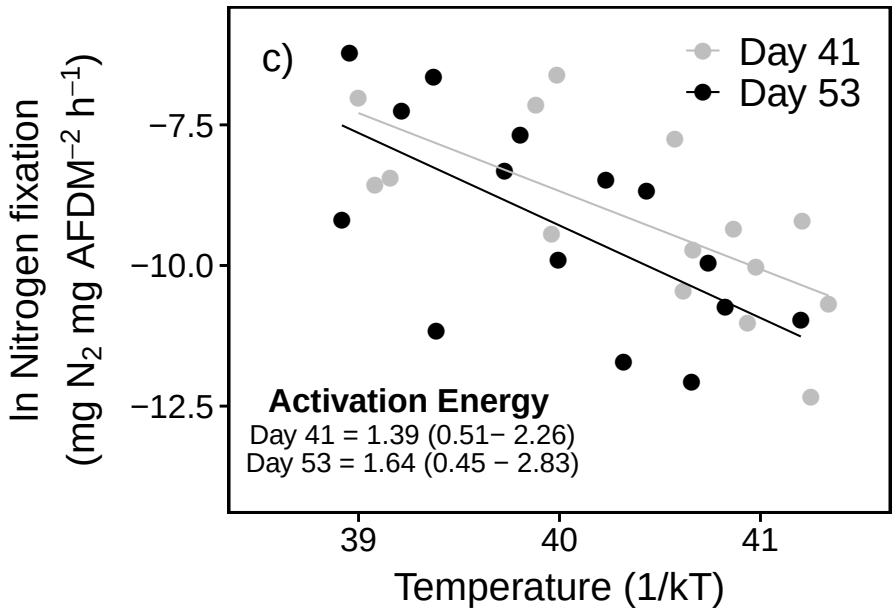
c)
Day 41
Day 53
ln Nitrogen fixation
(mg N_2 mg AFDM^{-2} h^{-1})
−7.5
−10.0
−12.5
Activation Energy
Day 41 = 1.39 (0.51− 2.26)
Day 53 = 1.64 (0.45 − 2.83)
39
40
41
Temperature (1/kT)